

# Investigations of a Pre-Swirl Cooling Air Flow System with Data Acquisition in the Absolute and Relative Frame of Reference

D. Weltersbach<sup>\*</sup>, D. Brillert<sup>\*\*</sup>, C. Cichon<sup>\*</sup>

<sup>\*</sup>Siemens Power Generation  
Wiesenstrasse 35  
45166 Mülheim  
Germany

<sup>\*\*</sup>Siemens Power Generation  
Kaiserleistrasse 10  
63067 Offenbach am Main  
Germany

**Abstract:** For further improvements in efficiency and performance of gas turbines, the secondary air system, i.e. the required cooling mass flow, plays an important role. The pre-swirled secondary air supply is a common method in the aero industry and is a promising option for heavy-duty gas turbine industry to reduce the air temperature for the blade supply and disc cooling.

In the experimental investigation reported here, a system with pre-swirl nozzles was run in a test rig. In the rotating system, static and total relative temperatures as well as relative pressures were measured. The disc and the receiver holes in the flow path entering the rotating system were instrumented. In the stationary system, pressures and temperatures were hooked up in the disc to casing cavities. All mass flows entering and leaving the test rig were measured by means of orifices.

The effectiveness of the cooling air was measured by changing the following parameters:

- disc velocity to swirl ratio
- pre-swirler geometry
- mass flow.

The experimental data show that a significant increase of cooling air performance, i.e. reduction of total air temperature in the relative frame, can be obtained in the system investigated. The measurements of the test rig confirm that the system effectiveness is basically a function of disc velocity to swirl ratio and pre-swirler pressure ratio. The effective pre-swirler velocity depends highly on the pre-swirler design.

A one dimensional model to calculate the relative pressures in the distribution holes of the rotor disc is applied to the measured data in consideration of disc friction put in the flow and a subsequent increase of total temperature. Calculated and measured pressures in the relative frame are compared.

**Keywords:** experimental investigation pre-swirler design, measurements relative frame, total temperature increase by disc friction, momentum and energy balance

## 1 Introduction

Investigations on pre-swirler systems have been carried out by others and had already proven the practicability of such a design. Among the first were Meierhofer and Franklin [1] who reported on measurements in a direct transfer system – i.e. a design whose characteristic is that the axis of the stator nozzles meet the rotor receiver holes at the same diameter. Meierhofer and Franklin ran tests with

different arrangements of nozzle sectors, rotor speeds and nozzle pressure ratios. The tests confirmed, by measuring the cooling air temperature in the rotating disc channels, that a significant reduction of cooling air temperature can be obtained. System effectiveness was found to be dependent on pre-swirl velocity ratio  $u/c$ , with  $u$  as the circumferential speed of the receiver holes and  $c$  as the effective discharge velocity of the nozzles.

Popp et al [2] performed flow field computation of a system with a coverplate in front of the receiver holes in the rotor. They determined that the most important parameter for efficiency is the ratio of receiver holes to nozzle area  $A_{rec}/A_n$  and suggested a proportion higher than 4.

Dittmann et al [3] performed tests on a pre-swirl test rig at the University of Karlsruhe with  $u=161$  m/s and found that the influence of relative inflow angle to the receiver holes on system performance was high. Discharge behaviour also depends on the number of the receiver holes and can be increased if a fillet radius is applied at the bore inlet. Continued experimental investigations of Geis et al [4] with the above mentioned test rig comprised thermocouple measurements with a high recovery factor in the receiver holes. Thereby cooling air temperature reduction in the relative frame of reference was measured and cooling efficiency for different pre-swirler pressure ratios and rotational speeds was derived. A model for viscous drag of the rotor was applied to the test results, and deviation of measured and theoretical cooling air temperature reduction were discussed with respect to rotor disc frictional work.

Further measurements with a modified experimental test set up of the Karlsruhe test rig have been reported by Dittman et al [5]. A torque meter was coupled to the shaft and, by determination of the rotor work, the velocity at the inlet of the receiver holes was analyzed. The losses of the nozzles, the pre-chamber and the receiver holes were separated. It was confirmed that the flow angle relative to the receiver hole axis has a strong influence on cooling air temperature reduction. Depending on this relative angle, an upstream influence on the discharge behaviour of the pre-swirler nozzles was found. Superimposing a radial outflow of disc cooling air on the pre swirled flow increased the cooling air temperature and thus diminished the effectiveness of the pre-swirl system.

Chew et al reported on measurements executed on another direct transfer pre-swirl test rig at the University of Surrey [6]. He concluded from the measurements that surface friction effects are quite small in the investigated design of the pre-swirl chamber. Losses through the nozzle accounted for a large portion of the rise in cooling air temperature compared to the ideal value. Chew et al also compared the experimental results of the test rigs in Karlsruhe and Surrey [7] in order to determine, why the performance of the Surrey test rig was higher. The

CFD model indicated that the primary cause of the difference was the moment imposed by the stator on the pre-swirled air, which depends on the wetted surface area of the pre-swirl chamber stator wall.

Owen et al [8] executed measurements on a pre-swirl test rig at the University of Bath. Owing to mixing losses between the nozzles and the receiver holes, a significant drop in total pressures was found. Discharge coefficients for the receiver holes were analyzed. They increased with higher flow rates and were lower than those obtained by other research workers.

This paper describes investigations carried out on a new direct pre-swirl system test rig. This test rig was built to investigate the potential cooling air reduction of such a design for Siemens combustion turbines by measuring pressures and temperatures in the rotating system. Design of the rig and testing conditions were chosen such that the results can be applied to heavy-duty gas turbine operation.

## 2 Experimental Set Up

In order to meet the requirements of similarity between testing conditions and full-scale gas turbine, disc circumferential speed and pre-swirl nozzle Mach-number were kept equal to the original terms. Figure 1 displays a schematic drawing of the test rig.

Mass flow to the test rig was provided by a screw type compressor. All mass flows leaving and entering the test rig are measured by means of orifices in the system. A DC motor drives the test rotor via a gearbox. The speed can be adjusted as required. Due to the high rotational speed, tilting pad bearings were chosen to support the rotor. The lube oil system beside the test rig is equipped with a main and a safety pump that feed the gearbox and the cooling air separation test rig. Automatic control is implemented by means of a Siemens Simatic programmable logic controller that monitors critical measured data like casing and shaft vibration, bearing temperatures, lube oil supply temperature and pressure, rotor speed and axial thrust.

Figure 2 shows a half section of the test rig and the rotor. Beside the gearbox end coupling is a disc on the rotor by which means the thrust acting on the rotor can be balanced in case the axial load capacity of the axial bearing is exceeded. The disc rim between the two tilting pad bearings is equipped with receiver holes which are flowed by cooling air. Channels through the disc and the rotor were provided for various sensing lines of the measuring points in the

rotating system. Beside the radial bearing is a telemetry ring that transmits the data out of the rotating system via radio to an antenna in the absolute frame of reference.

The horizontal split-welded casing carries the pre-swirler and adjustment rings which separate different cavities. The rings can be moved axially thereby changing the stator to rotor axial clearance. Several holes in the casing shell enable to flow cavities in order to control friction induced temperature rise at high speed and to feed labyrinth seals with pressurized shop air to reduce leakage between adjacent cavities. Main flow enters the pre-chamber of the test rig through 4 flanges and passes into the rotor stator annulus via the pre-swirler which generates angular momentum in the direction of rotor rotation. The area ratio  $A_{rec}/A_n$  is 2,8. The pre-swirler is of ring design and is exchangeable.

Whereas the main part of the flow leaves the annulus into the receiver holes in the disc rim, a certain amount of leakage air flows through the labyrinth seal located on the balcony protruding the disc head. The item in Fig. 2 shows a magnification of this area. The flow leaving the receiver holes enters the main blow-off cavity and then leaves the shell. The leakage air which enters the front blow-off cavity is separated from the receiver outflow by a sealing blow-

off ring with labyrinth seals. Within the scope of measurements reported here, no sealing air was fed to the sealing blow-off ring. Figure 2 displays the notation for cavities and the flow path of the incoming air.

To ensure test bed safety under all conditions, casing wall thickness, joint bolting, casing support and foundation were designed to control the worst case scenario of a rotor rupture. Figure 3 shows the test rig and Fig. 4 the rotor.

**Instrumentation**

To monitor the pressures and temperatures in the test rig, various measurement points were provided in the rotating and non-rotating system. Table 1 summarizes the implemented sensors. Figure 2 shows an arrangement of the main test points. In every cavity, radial and circumferential distribution of flow temperature and pressure are hooked up. Pressures are measured by means of multiple channel PSI modules and robust Rosemount transducers. K-type thermocouples are used to measure temperatures.

In the rotating system, new pressure sensors, capable of resisting centrifugal load even at the disc rim at high speed, were positioned at different points.

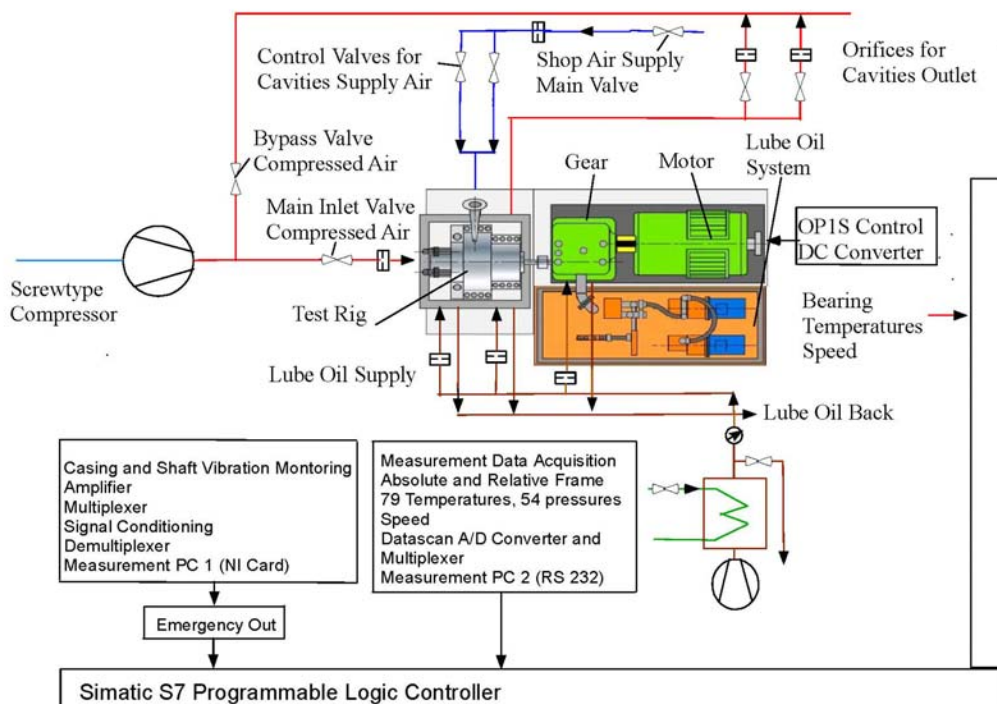


**Fig. 1: Schematic Drawing**

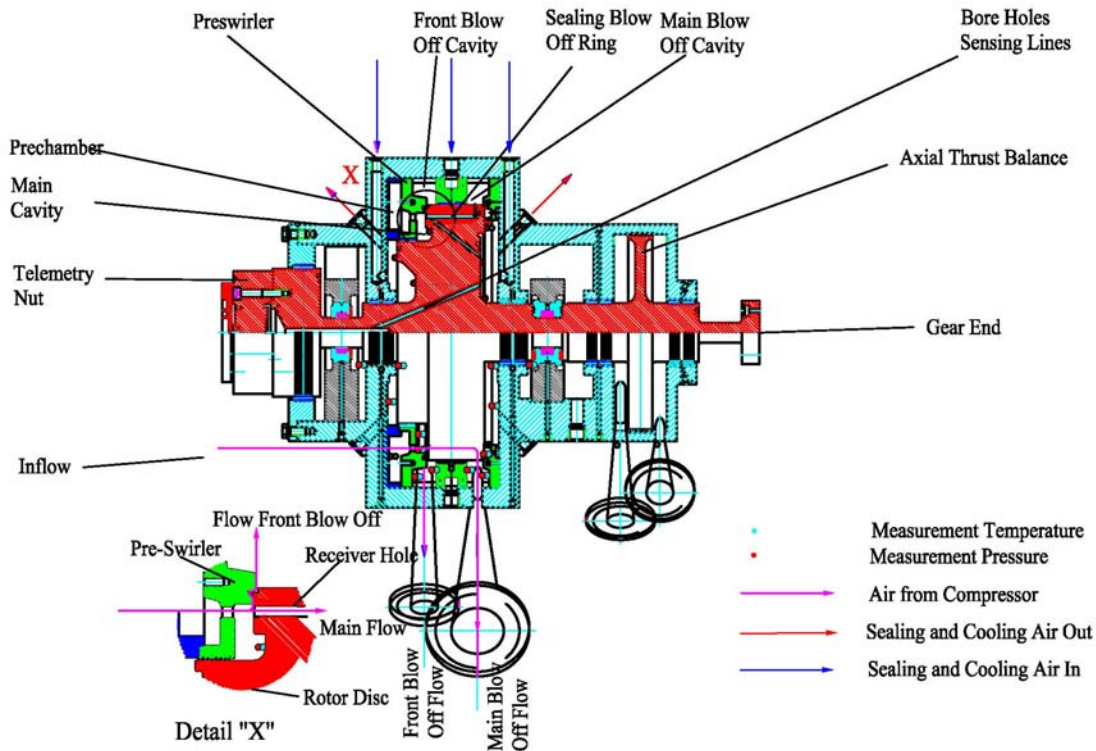


**Fig.2: Half Section Of Test Rig**



**Fig. 3: Test Rig**

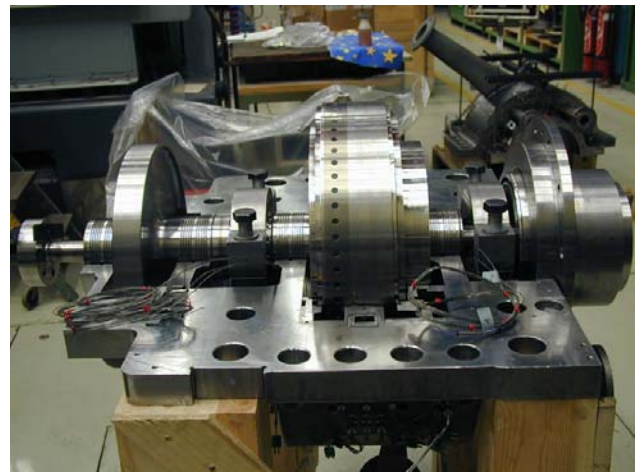


**Fig. 4: Test Rotor**

Figure 5 displays one of the sensors at a receiver inlet. In order to have a back-up solution for these new sensors, redundant pressure sensors were mounted on the shaft centerline beside the telemetry ring. Pressure data taken with these sensors however, have to be adjusted for centrifugal load on the air in the pressure sensing line between disc head and shaft centerline. Operational experience with the sensors directly located at the disc head, proved the practicability of the redundant sensor implementation. After shaft balancing, 2 of the 6 sensors failed and within a short time of test operation, most of the sensors fall out.

The main purpose of the pre-swirl system is to achieve a total air temperature reduction in the relative frame of reference. Therefore temperature measurement of the flow in the receivers was one of the most important parameters of the test set up. Two receiver holes were equipped with sleeves carrying thermocouples directed against flow thereby ensuring a high recovery factor. Figure 6 shows a sleeve with the instrumented thermocouple.

The margin of error for the different sensors were:  
 Thermocouples for air temperature  $\pm 1\text{K}$   
 pressures in the absolute frame  $\pm 0,25\%$   
 pressures in the relative frame  $\pm 4\%$  (range).



**Fig. 5: Pressure Sensor At Receiver Inlet**

Table 1

sensor	rotor	stator
material temperature	28	-
air temperature	7	52
static pressure	-	34
total pressure	6	-

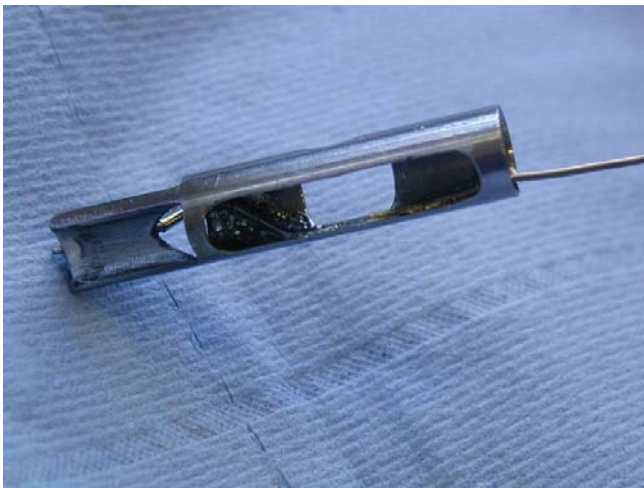


**Fig. 6: Rotor Bore Holes Sleeve with TC**

### 3 Results and Discussions

Two set ups with different pre-swirler design are within the scope of measurements reported here. Figure 7 displays a pre-swirler with vanes (PSV) and Fig. 8 one with distribution holes (PSB). Total flow area, outlet angle and the distance from swirl nozzle flow path to rotor axis were equal. The test program was to run the rotor at various speeds thereby changing the pre-swirler pressure ratio  $\pi_{PSV} = p_1/p_{t10}$  from 0,91 to 0,66.

Figures 9 and 10 show the total temperature drop from pre-chamber to receiver holes in the rotor in relation to the total temperature in the pre-chamber. The temperature rise that would be experienced if the inflow to the rotor was without swirl coaxial to the rotor axis is  $u_1^2/(2*c_p)$ . Measurements with axial flow on the nozzle exit

were not part of the test program. Such investigations however had already been done by Meierhofer et al [1] proving that the expected temperature increase under these conditions was realistic. The scaling of ordinate and abscissa in both diagrams were the same. This is the case of all figures presented in this paper, if a comparison between different experimental set ups, namely PSV and PSB, is made. The graphs in both diagrams display that the temperature drop depends on pre-swirler pressure ratio and rotational speed. High pre-swirler pressure ratios lead to high reduction of total temperature in the relative frame of reference. At the lowest pressure ratio, a temperature rise was observed. Temperature reduction for a given pressure ratio bottoms out at a certain speed which is shifted up if the pre-swirler pressure ratio is increased. Comparison of PSV and PSB data show significant higher temperature drops and a better performance for the vane type pre-swirler.

A one dimensional theoretical model of the flow predicts relative total temperature in the receiver bore holes  $T_{t2'th}$  to

$$T_{t2'th} = T_{0t} + \frac{u_1^2 - 2u_1c_{1tis}}{2c_p} \tag{1}$$

with the total temperature in the pre-chamber  $T_{0t}$ , receiver holes circumferential speed  $u_1$  and tangential component of isentropic nozzle discharge velocity  $c_{1tis}$ . Equation (1) applies to a system that has the same receiver hole and pre-swirler radius which is the case in test set up described in this paper. This equation shows that the rotor “sees” a lower air temperature than the pre-chamber in the range of  $0 < u_1 < 2 * c_{1tis}$ . To use this effect for advanced cooling schemes of modern gas turbines, engineering efforts on pre-swirl systems design is needed. From equation (1) it follows that temperature drop  $T_{t2'th} - T_{0t}$  is at a minimum for  $u_1 = c_{1t}$  and higher and lower values of  $u_1$  will lead to smaller temperature drop in the rotor bore holes compared to this value.

Figure 11 depicts a comparison of measured and theoretical temperature drop according to the equation (1) for both pre-swirler designs. The data shows that there is a significant gap between theoretical and calculated temperature reduction and that the vane type pre-swirler performs better compared to the bore type design. This difference between theoretical and measured data of a pre-swirl system had already been discussed by Geis et al [4]. The curve displaying calculated values derived from equation (1) assumes isentropic expansion from the pre-chamber to the main cavity and neglects losses in stator rotor annulus and at the inlet from the receiver. Beyond this, the flow field in the main chamber is

highly 3 dimensional and leakage flows across labyrinth seals are superimposed on the nozzle inflow. Mixing and transposition of angular momentum from the pre-swirled air entering the main cavity are affected by the nozzle number and diameter as well as main chamber geometry. Therefore losses of different origin must be considered. The discharge coefficient of both the investigated pre-swirl stator rings, as previously carried out cold flow tests outside the test rig with pressurized shop air have proven, depends on the geometry of the swirl nozzles. These tests confirmed that the vane type pre-swirler shows better discharge characteristics. Meierhofer et al [1] stated that the qualitative effect of nozzle height and through flowed circumference of nozzle ring is such, that reduced nozzle heights increase secondary flow and an decrease of open circumference leads to increase of losses due to blockage effects. With regard to all three points the vane type pre-swirler is superior to the bore type one. The experimental data confirm the above- mentioned considerations.

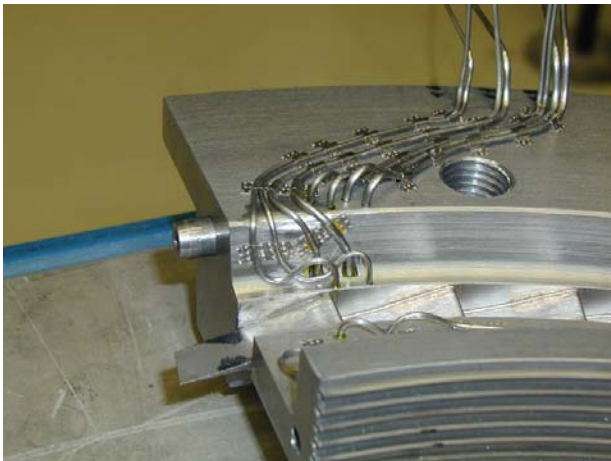


**Fig. 7: Pre-Swirler with Vanes (PSV)**



**Fig. 8: Pre-Swirler with Distribution holes (PSB)**

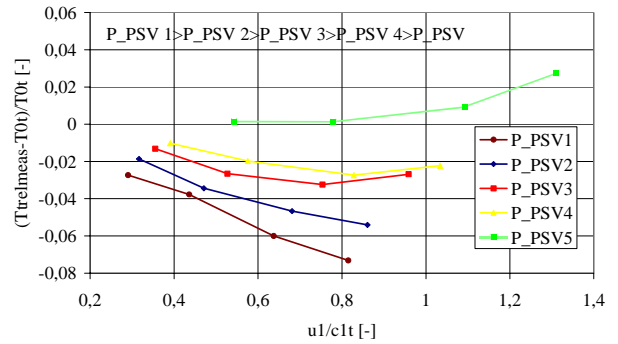


**Fig. 9: Relative Temperature Drop PSV**

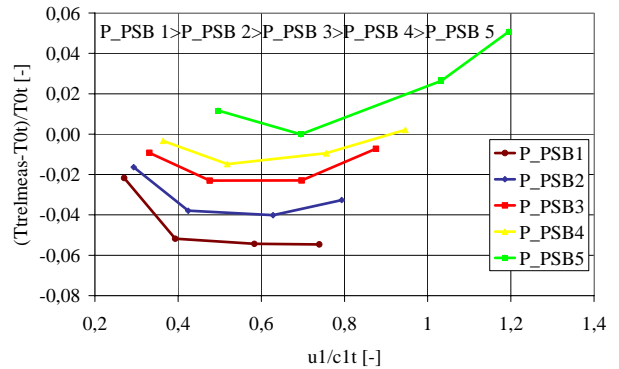


**Fig.10: Relative Temperature Drop PSB**

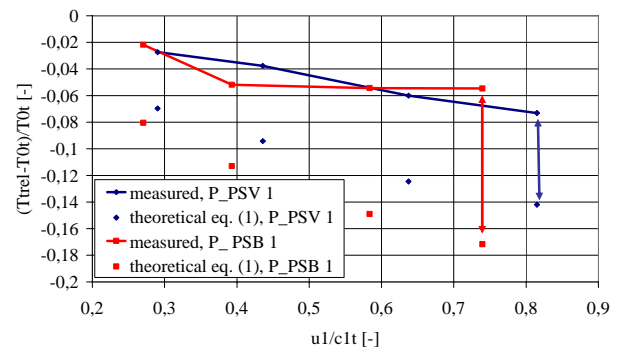


**Fig. 11: Temperature Drop PSV and PSB**

Geis et al [4] discussed potential sources for the performance decrease. They remarked that the effects in the main cavity seem to be of great importance to the drastic differences of a real system to one operating under isentropic conditions. Equation (1) assumes constant total temperature in the pre-chamber and the main cavity. The effect of viscous drag between flow and disc depend on mean tangential velocity in the main chamber and rotational speed of disc however. If the disc speed is higher than the tangential velocity of the air in the main cavity, total temperature in the main cavity is increased due to disc work. These effects must be considered and Geis et al [4] were among the first to outline the impact of viscous drag from the rotor on total temperature in the main cavity. To rate the potential increase of total temperature in the rotor stator annulus downstream from the pre-swirler, energy balance for the main chamber has to be given. This yields

$$\Delta T_{t1} = \frac{M_{rot} \omega}{m c_p} \quad (2)$$

with

$$T_{t1} = T_{0t} + \Delta T_{t1} \quad (3)$$

$\Delta T_{t1}$  is the temperature increase caused by viscous drag of the rotor moment  $M_{rot}$ . Geis et al [4] calculated the drag work of the disc following an analytical solution for  $M_{rot}$  presented by Goldstein (1935). This method assumed stationary turbulent flow with boundary layers according to the  $1/7^{th}$  power law and neglected pre-swirl jets and rotating disc holes. Their result was that frictional heating plays an important role at high rotational disc speed and low cooling flow rates which result subsequent at low pre-swirler pressure ratios. The highest value for  $\Delta T_{t1}$  calculated for  $\pi_{psv} = 1,1$  was 2 K at the highest rotor speed run in the tests from Geis et al [4]. In this paper, a modified attempt to include momentum and energy balance in the analysis of disc friction is used. This will be reported on in detail later.

Figures 12 and 13 show cooling efficiency defined as

$$\eta_{cool} = \frac{T_{0t} - T_{t2' meas}}{T_{0t} - T_{t2' th}} \quad (4)$$

for the investigated pre-swirlers. Negative efficiencies indicate temperature increase in the rotating system which was observed for low pre-swirl pressure ratios as already outlined. The Figs. depict again that high pressure ratios are a prerequisite for high cooling performance and that the vane type pre-swirler shows better results. The X-axis is the ratio of receiver bore hole circumferential speed to tangential velocity at nozzle exit. Maximum performance following equation (1) is to be expected for a ratio of 1 which is not the case as both figures show. One possible explanation is that the average tangential velocity in the main chamber is lower than at the nozzle exit. This reduces the potential temperature reduction in the relative frame and shifts the curve peaks to lower speed ratios.

Geis et al [4] performed PIV measurements in a pre-swirl chamber and reported that velocity in the main chamber was about 50% lower than for calculated reversible flow at the nozzle exit. Their experimental set up however featured a comparatively small nozzles number (12) whereas in the test set up reported in this paper the open circumference of the pre-swirler ring in both geometrical configurations is much higher compared to that. The vane type pre-swirler carries one discharge vane segment beside the other. Although this effect should therefore be of lower importance in the given case, it may still be present. It appears from Figs. 12 and 13 that the PSV efficiency peaks are

closer to the theoretical limit of  $u_1/c_{1tis} = 1$  in general compared to those of the PSB swirler. Moreover, it turns out that increasing pressure ratios shift the mismatch between theoretical limit and maximum to higher values, which is obviously not the case for the PSV.

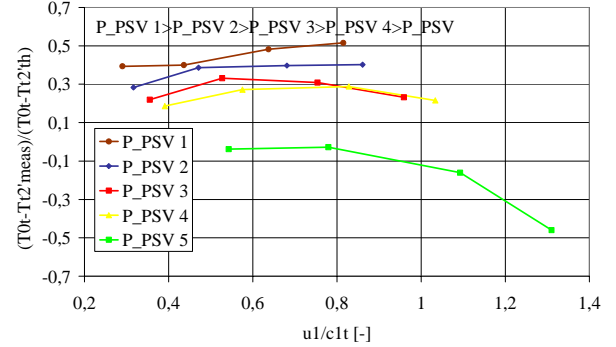


Fig. 12: Cooling Efficiency Preswirler PSV

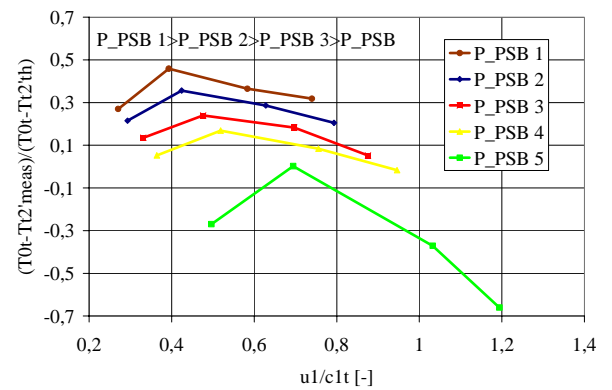


Fig. 13: Cooling Efficiency Preswirler PSB

The measurement data reported here cover total pressures which were taken at the receiver bore holes of the rotor. Figure 14 displays measured total relative pressures  $p_{t2' meas}$  as a function of inflow angle to the receiver holes and pre-swirler pressure ratio for the vane type swirler. Theoretical total pressures assuming adiabatic reversible conditions with

$$\frac{p_{t2' th}}{p_{t0}} = \left( \frac{T_{t2' th}}{T_{t0}} \right)^{\frac{\kappa}{\kappa-1}} \quad (5)$$

were added for reference. The theoretical pressure data are significantly higher than the measured data, indicating that the inflow suffers relevant losses and that equation (5) over-predicts total relative pressures. The receiver holes in the existing test set up are long enough to ensure a uniform distributed velocity profile at the position where total pressures are measured even for  $u_1/c_{1tis} \neq 1$ . Since pressure measurements in the relative frame of reference are difficult to perform and require great care and experimental experience during installation, the question had to be answered whether the measured pressure data was reliable. To find a supplementary way to calculate the receiver pressures, static

pressures picked up in the main blow off cavity directly behind the receiver holes outlet were used. To account for receiver hole pressures, mass flow rate had to be determined from the measured data. This quantity had not and could not been measured directly. Leakage flows crossing the labyrinth seals had to be analysed in order to perform a mass balance on the cavities connected to the receiver holes.

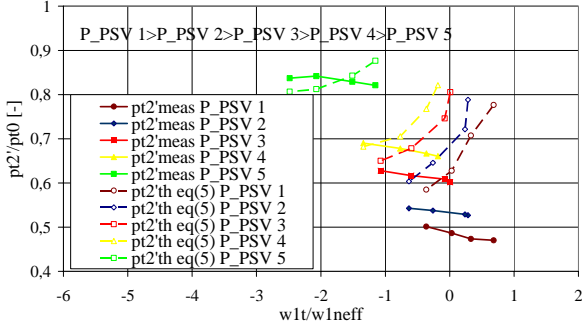


**Fig. 14: Measured Pressures in Receiver Holes PSV**

This balance was performed using measured wall static pressures to calculate labyrinth leakages with a well established analytic procedure within Siemens PG, already proven in combustion and steam turbines. All inlet and outlet flows to the test rig were measured with orifices. This balance done for the main cavity and main blow-off cavity, independently determined a mass flow at the receiver inlet and outlet, that were both well in accordance with each other. Applying an approach suggested by Kutz et al [9], relative total pressure in the receiver holes was calculated using the static pressure in the main blow-off cavity and the bore hole mass flow.

With

$$\frac{\dot{m} \sqrt{T_{t2''}}}{A_{receiver} p_{s2}} = \sqrt{\frac{2\kappa}{(\kappa-1)R} \left( \left( \frac{p_{t2''}}{p_{s2}} \right)^{\frac{2(\kappa-1)}{\kappa}} - \left( \frac{p_{t2''}}{p_{s2}} \right)^{\frac{\kappa-1}{\kappa}} \right)} \quad (6)$$

the inverse function for  $p_{s2}/p_{t2''} \geq 2/(\kappa+1)^{\kappa/(\kappa-1)}$  is

$$p_{t2''} = p_{s2} \left( \frac{1}{2} + \sqrt{\frac{1}{4} + \left( \frac{\dot{m} \sqrt{T_{t2''}}}{A_{receiver} p_{s2}} \right)^2 \frac{(\kappa-1)R}{2\kappa}} \right)^{\frac{\kappa}{\kappa-1}} \quad (7)$$

The quantities  $T_{t2''}$  had to be derived from the measured variable  $T_{t2',meas}$  by considering the work transmitted to the flow by the rotor due to the radius difference between receiver holes and disk rim as Fig. 2 depicts.

Figure 15 shows the calculated  $p_{t2'}$  data in comparison to the measured data.  $p_{t2'}$  data were determined following equation (7) and considering rotor work transmitted to the flow between distribution holes radius and disk rim. The Fig. indicates that the measured relative pressures

correspond closely to the static wall pressures taken at the receiver outlet. The discrepancy between theoretical total receiver hole pressure according to equation (5) and the measured ones, appears to be caused by pressure losses in the main cavity.

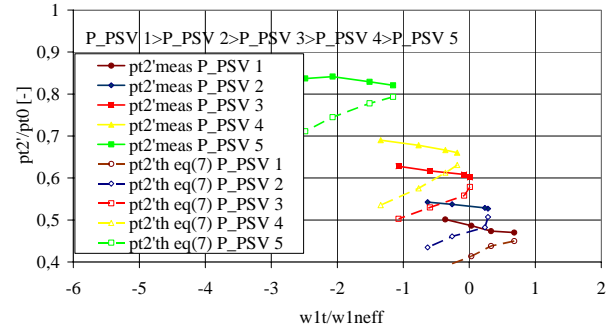


**Fig. 15: Measured and Calculated Total Pressures in Receiver Holes PSV**

As previously discussed, disc friction put in the flow by friction is calculated following a suggestion from Kutz et al [9], which includes momentum and energy balance in the analysis of total temperature increase in the main chamber. Momentum balance on the flow in the main chamber is given by

$$\dot{m} r_{receiver} c_{1teff} - \dot{m} r_{psn} c_{1t} = M_{rot} + M_{stat} \quad (8)$$

with

$$M_{stat} = -A_{stat} r_{stat} C_{Mstat} \frac{\zeta}{2} c_{1teff}^2 \quad (9)$$

$$C_{Mstat} = C_{stat} \left( \frac{c_{1teff} r_{stat}}{v} \right)^{-0.2} \quad (10)$$

$$M_{rot} = \text{sign}(u - c_{1teff}) A_{rot} r_{rot} C_{Mrot} \frac{\zeta}{2} (u - c_{1teff})^2 \quad (11)$$

$$C_{Mrot} = C_{rot} \left( \frac{|u - c_{1teff}| r_{rot}}{v} \right)^{-0.2} \quad (12)$$

$C_{Mstat}$  and  $C_{Mrot}$  denote a friction coefficient derived from boundary layer equations for turbulent flow. These coefficients either account for the moment required to turn a disc relative to flow ( $C_{Mrot}$ ) or to fix a non rotating disc if the flow is turning ( $C_{Mstat}$ ). In both cases the relative speed between flow and disc is applied. In equation (11) the abbreviation ‘‘sign’’ stands for the function signum.  $c_{1teff}$  denotes an effective tangential velocity in the main chamber.

If equations (9)-(12) are inserted into equation (8) with the additional assumption  $c_{stat}=c_{rot}$  a first equation for  $M_{rot}$  is derived from momentum balance



$$\frac{M_{rot}}{m} = \frac{r_{receiver} c_{1teff} - r_{Psn} c_{1t}}{\left[ 1 - \text{sign}(u - c_{1teff}) \frac{A_{stat}}{A_{rot}} \left( \frac{r_{stat}}{r_{rot}} \right)^{0,8} \frac{c_{1teff}^{1,8}}{(u - c_{1teff})^{1,8}} \right]} \quad (13).$$

Energy balance for the flow was already given with equation (2) and (3). Modification of equation (1) such that measured relative total temperature is used to define an effective tangential velocity in the main chamber leads to

$$T_{t2'meas} = T_{t1} + \frac{u^2 - 2uc_{1teff}}{2c_p} \quad (14)$$

Applying equation (14) to (2) and (3) derives a second term for  $M_{rot}$  on the basis of energy balance

$$\frac{M_{rot}}{m} = \frac{1}{\omega} \frac{u^2}{2} \left[ \left( \frac{c_{1teff}}{u} - 1 \right) - \frac{2c_p (T_{0t} - T_{t2'meas})}{u^2} \right] \quad (15).$$

In (14) and (15) all quantities except  $c_{1teff}$  were measured or are well defined. With a numerical solver it is possible to calculate  $c_{1teff}$  and hence to determine  $T_{t1}$  and  $M_{rot}$ . Figures 16 and 17 depicts the determined total temperature increase due to windage for PSV and PSB. The curves show that windage heat plays a significant role at high disc rotational speeds and low pre-swirler pressure ratios. To explain the performance discrepancy between a real pre-swirler system, and one showing isentropic qualities, for those conditions which are of practical importance for heavy gas turbine operation, i.e. high pressure pre-swirler ratios, there is no evidence. In order to avoid reverse hot gas flow back into the cooling air system, low pre-swirler pressure ratios, namely in the first turbine stage, are not possible.

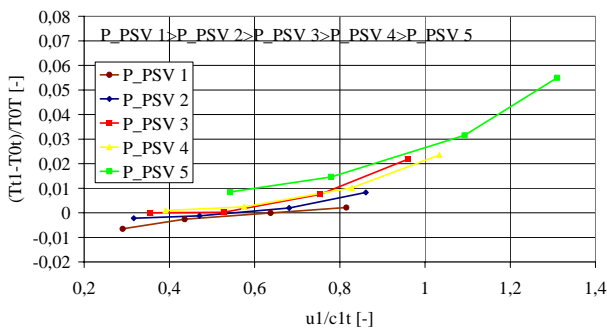


Fig. 16: Temperature Rise Due to Windage PSV

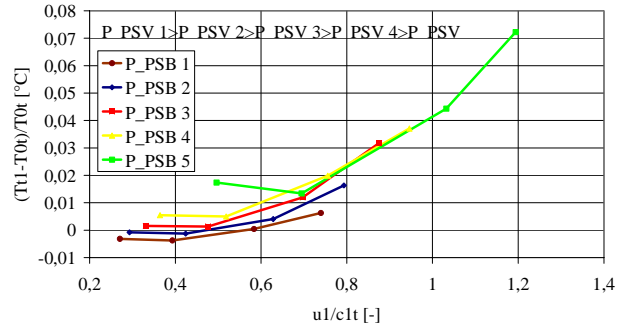


Fig. 17: Temperature Rise Due to Windage PSB

### 4 Conclusion

In this paper the new test rig at Siemens PG was presented. The purpose of this test rig is to examine new cooling air schemes, particularly pre-swirler systems which are a promising option for modern heavy-duty gas turbines. Within the scope of measurements reported here are two different geometric configurations of pre-swirler with identical flow area, nozzle exit angle and nozzle flow path distance to rotor axis, but different nozzle configurations. Whereas the first swirler was designed with vane segments, the second had nozzle holes of cylindrical form. Temperature and pressures were picked up in the absolute and relative frame of reference, and signals were transmitted out of the rotating system via antenna. The data obtained show that cooling performance, i.e. cooling air temperature reduction in the rotating system, was significantly better for the vane type pre-swirler. Temperature decrease in the receiver bore holes is a function of pre-swirler pressure ratio and the scale of rotor disc circumferential speed to nozzle discharge velocity. The measured data show that the effective tangential velocity at the inlet of the receiver bore holes is clearly smaller than at the nozzle discharge. Thus it is confirmed, that the losses through the nozzle are one important factor for the rise in cooling air temperature. The pressures measured in the relative frame of reference are significantly lower than expected for isentropic flow. Recalculations executed with the static exit pressure of the receiver holes and the cooling air mass flow however indicated that the measured pressures are realistic and thus pressure losses, namely in the main cavity and at the inlet of the receiver bore holes, are genuine. A new approach, analysing total temperature increase due to viscous drag of the rotor, was applied using angular momentum and energy balance for the main cavity. The numerically solved equations however, show that this effect is significant only for high disc speed and low tangential flow velocity in the denoted cavity. Future engineering efforts are necessary to analyse potential sources of pressure losses for 3

dimensional flow in the rotor stator annulus between pre-swirler and rotor.

**Nomenclature**

- A flow area
- $C_M$  friction coefficient
- M moment
- R gas constant air
  
- c velocity
- $c_p$  specific heat
- $c_t$  tangential component of velocity
- $\dot{m}$  nozzle exit discharge mass flow
- p pressure
- r radius
- t temperature
- u circumferential speed
  
- $\eta_{cool}$  cooling efficiency
- $\omega$  disc angular velocity
- $\zeta$  density flow
- v viscosity
- $\kappa$  adiabatic exponent

**Subscripts**

- is isentropic
- meas measured
- n nozzle
- psn pre-swirl nozzle
- rec receiver
- rel relative frame of refernce
- rot rotor
- s static
- th theoretical
- stat stator
- t total
- 0 prechamber
- 1 main cavity
- 2' receiver holes rotor disc
- 2'' rotor disc rim
- 2 main blow off cavity

**References**

[1] Meierhofer, B., Franklin, C.J., „An Investigation of a Preswirled Cooling Airflow to a Turbine Disc by Measuring the Air Temperature in the Rotating Channels”, *ASME Paper 81-GT-132*, 1981

[2] Popp, H., Zimmermann H., Kutz J., 1998, „CFD Analysis of Coverplate Receiver Flow”, *Journal of Turbomachinery*, Vol. 120, page 43, 1998

[3] Dittmann, M., Geis, T., Schramm, V., Kim, S., Wittig, S., 2002, “Discharge Coefficients of a Preswirl Sytem In Secondary Air System”, *Journal of Turbomachinery*, Vol. 124, page 119

[4] Geis, T., Dittmann, M., Dullenkopf, K.,

„Cooling Air Temperature Reduction in a Direct Transfer Preswirl System”, *ASME Paper 03-GT-38231*, 2003

[5] Dittmann, M., Dullenkopf, K., Wittig, S., „Direct-Transfer Preswirl System; A One Dimensional Modular Characterization Of The Flow“, *ASME Paper 03-GT-38312*, 2003

[6] Chew, J.W., Hills, N.J., Khalatov, S., Scanlon, T., Turner, A.B., „Measurement And Analysis Of Flow In A Pre-Swirled Cooling Air Delivery System”, *ASME Paper 03-GT-38084*, 2003

[7] Chew, J.W., Hills, N.J., Ciampoli, F., S., Scanlon, T., “Pre-Swirled Cooling Air Delivery System Performance”, *ASME Paper 05-GT-68323*, 2005

[8] Owen; J. M., Yan, Y., Lock, G.D., Gord, M.F., Wilson, M., “Fluid Dynamics Of A Pre-Swirl Rotor-Stator System”, *ASME Paper 02-GT-30415*, 2002

[9] Kutz, J., 2003, *Internal Statement ICAS GT Work Group*